Available online at www.sciencedirect.com

ScienceDirect

Procedia Structural Integrity 51 (2023) 51–56

Structural Integrity Procedia

www.elsevier.com/locate/procedia

6th International Conference on Structural Integrity and Durability (ICSID 2022)

A numerical study on tensile stress concentration in semi-ellipsoidal corrosion pits

F. Mehri Sofiani[a,*], S. Chaudhuri[b], S. A. Elahi[a], K. Hectors[a], W. De Waele[a]

[a]*Ghent University, Department of Electromechanical, Systems and Metal Engineering, Soete Laboratory, Technologiepark-Zwijnaarde 46, 9052, Zwijnaarde, Belgium*

[b]*Bundesanstalt für Materialforschung und -prüfung (BAM), Berlin, Germany*

Abstract

Pitting corrosion is a common cause of concern for steel structures in an offshore environment. As geometric stress-concentrating features, corrosion pits can potentially act as fatigue crack initiation sites. The severity of a pit can be analyzed based on its geometric characteristics, and the loading and boundary conditions of the component. In this study, the stress distribution in and around a semi-ellipsoidal pit in a plate subjected to (remote) uniaxial tension is investigated using finite element analysis. The investigated characteristics include the width, length and depth of semi-ellipsoidal pits ($2b$, $2c$ and a, respectively); the remote load acts parallel to the pit length. A parametric study was conducted with a focus on normalized parameters b/c, a/t and $a/2c$, and their effect on the stress concentration factor (SCF). The considered value ranges for b/c, a/t and $a/2c$ were 0.1 to 1, 0.01 to 0.2 and 0.125 to 1.5, respectively. Within the range of values for each parameter, SCF did not vary significantly with changes in a/t and increases for increasing $a/2c$ and b/c values. The maximum value of SCF is obtained for the sharpest pit with a circular mouth ($a/2c$ = 1.5 and b/c = 1).

Keywords: Stress concentration; pitting corrosion; linear elastic study; finite element analysis

* Corresponding author. Tel.: +32-9-331-0489
E-mail address: farid.mehrisofiani@ugent.be

10.1016/j.prostr.2023.10.066

1. Introduction

The global world population is expected to increase by 20% until the year 2040 based on the Stated Policies Scenario (IEA, 2019). Consequently, the energy demand may rise by 26% by 2040 (IEA, 2019). The crucial effect of climate change and the detrimental impact of air pollution on the Earth's ecosystems, are the major reasons to deploy renewable energy resources. Among these, offshore wind turbines (OWTs) represent promising technology for energy generation which convert wind energy into electricity. As the number of offshore wind farms rises, concerns regarding the OWT's structural integrity (Shittu et al., 2020) rise as well. The OWT support structures are subject to corrosion due to seawater and humidity (Adedipe et al., 2016). There are multiple types of corrosion (Ahmad, 2006) and pitting corrosion is one of the most insidious forms of localized corrosion. Additionally, OWT support structures undergo fatigue loads due to wind and waves. The combination of these damage mechanisms is generally categorized as corrosion-fatigue (Ahn et al., 1992; Zhang et al., 2018). The high cycle fatigue regime is applicable to OWT structures (Kolios et al., 2014). For such applications, stress-life (S-N) plots are used to assess the fatigue life. Fatigue life of structural components is affected by several factors such as their geometry, loading type, surface condition and environment. As corrosion pits act as stress raisers, fatigue cracks most likely initiate at pits (Farhad et al., 2021), though the influence of degraded material properties due to corrosion cannot be discounted (Vukelic et al., 2022).
This study is part of the MAXWind project with the main goal of rendering optimized inspection and maintenance plans for OWT structures. Hereto, an integrated corrosion-fatigue numerical model is being developed. The present study focuses on the pit-to-crack transition stage by investigating the stress concentration factor (SCF) for different pit configurations. The SCF can be used to quantify the stress raising effect of a pit, effectively allowing quantification of the severity of the pit geometry with respect to fatigue cracking.

Cerit et al. (2009) studied the stress distribution in pits with circular mouth in a plate subject to tensile and torsional (Cerit, 2013) loads. They reported SCF values according to the absolute size of the pit depth and the ratio of pit depth over pit mouth diameter. Further, they studied the effect of a secondary small pit at the bottom of a hemispherical pit. Huang et al. (2014) performed a similar study without considering the plate thickness effect on the stress concentration factor, but focusing on the effect of the pit mouth aspect ratio. An et al. (2019) conducted a numerical analysis of tensile stress concentration in a semi-ellipsoidal pit by taking the plate thickness into account in addition to pit depth over pit length ratio. However, they have not studied the effect of pit mouth aspect ratio on SCF. Shojai et al. (2022) have performed a probabilistic modelling of pitting corrosion to assess its influence on SCF in OWT structures. They evaluated the effect of interaction between two pits on SCF, and also reported SCF values for a few single pit configurations considering absolute pit depth size and pit half-length over depth ratio. Liang et al. (2019) investigated the effects of absolute pit depth size and half-length of pit on SCF. They located the pit at the centre of the top plate surface as well as the edge of the plate. None of these last two works have incorporated pit mouth aspect ratio in the model. In a preceding study (Mehri Sofiani et al., 2023), the effect of pit depth over pit length, pit mouth aspect ratio, local thickness loss and loading direction on SCF was studied. Also, the most critical regions within semi-ellipsoidal pits as the potential locations for crack initiation were identified. However, the effect of local thickness loss lower than 0.1 is not explored.

Adding to the state-of-the-art, the present work considers the combined effects of pit mouth aspect ratio, the pit depth over pit length ratio, and the plate thickness effect on SCF. Also, response of the material for local thickness loss lower than 0.2 is studied which is another novelty of the work.

Nomenclature

a	pit depth
b	pit mouth half width
c	pit mouth half length
L	plate length
t	plate thickness
OWT	offshore wind turbine
SCF	stress concentration factor
$\sigma_{nominal}$	nominal stress applied to the pitted plate
σ	principal stress at pit

2. Finite element model

For the linear elasto-static stress analysis, commercial software ABAQUS® v2021 was used. The finite element model consists of a square plate with a central pit at its top surface, see Fig. 1.

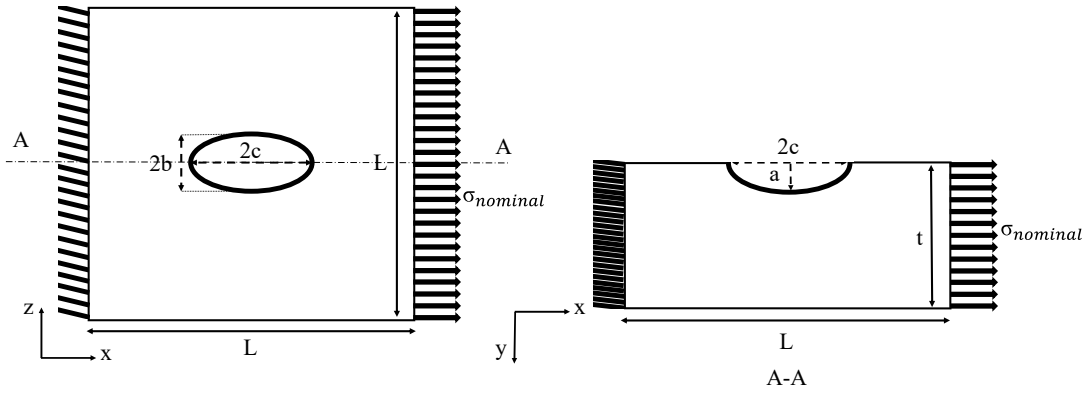

Fig. 1. Schematic representation of the pitted plate: top view of the plate (left) and through-thickness view of the plate (right).

As exhibited in Fig. 2, the 3D pitted plate is generated in ABAQUS® and exported as a .sat file containing three-dimensional geometry information. The exported file is then imported into the commercial meshing software Coreform Cubit® 2020.2 to mesh the pitted plate. Due to the rather complex geometry of the pits, the quadratic tetrahedral element type was adopted for meshing. Fig. 3 shows a cross-sectional view of a semi-spherical pit ($a/2c = 0.5$ and $b/c = 1.0$) where $a = b = c = 3$ mm and a fine mesh size of 0.01 mm was applied to the concave surface of the pit. In order to maintain a smooth transition from this fine to the global coarser mesh, a cubic partition is created at the vicinity of the pit and its edges are meshed with relatively larger mesh size of 0.5 mm. A global, coarser mesh size of 12 mm was also applied to the plate edges to reduce the computational costs. An .inp file consisting of the meshed 3D part is next exported from Coreform Cubit® and imported into ABAQUS®.

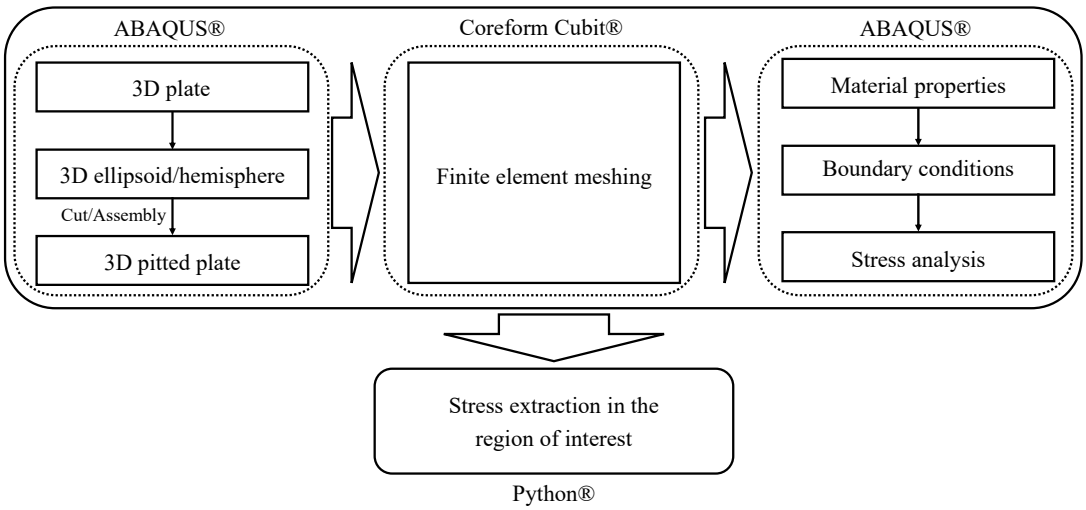

Fig. 2. Modelling and implementation process.

At this stage, the load and boundary conditions are added to the model. The pitted plate is subjected to a uniform axial tensile stress at one side and fixed at the opposite side; see Fig. 1. For the elastic material used in the simulations, a Young's modulus of 205 GPa and a Poisson ratio of 0.29 are used (Igwemezie et al., 2019). Ultimately, the stress analysis is performed and the output files are post-processed using Python. The post-processing extracts the principal stresses from the pit region to calculate the SCF which is defined as:

$$\text{SCF} = (max(\sigma_i)) \; / \; \sigma_{nominal} \tag{1}$$

where $\max(\sigma_i)$ is the maximum value of the principal stresses extracted from the region containing the pit and $\sigma_{nominal}$ is the nominal stress applied to the pitted plate. The entire modelling and implementation process shown in Fig. 2 was automated using ABAQUS scripting with Python.

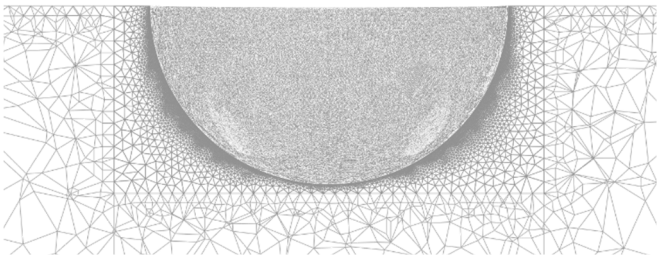

Fig. 3. FE mesh at semi-spherical pit.

This study investigates the effect of normalized geometric parameters of a corrosion pit on its SCF. This includes the ratio of pit semi-width over pit semi-length (b/c), the ratio of pit depth over pit length ($a/2c$), and the effect of localized thickness loss (a/t). Normalized parameters have been used to avoid being constrained to absolute dimensional values. Values of $a/2c$ equal to 0.125, 0.5, 1, and 1.5 were considered to address both wide and narrow shapes of a corrosion pit. Additionally, the pit mouth aspect ratio b/c was considered to be 0.1, 0.5, and 1.0. The value of 0.5 for $a/2c$ represents a hemispherical pit at b/c = 1. The model also incorporates a/t values of 0.01, 0.05, 0.1, 0.15, and 0.2.

3. Results and discussions

Fig. 4, exemplarily, shows the distribution of maximum principal stress for a plate with two different pit configurations. One having normalized dimensions a/t = 0.2, b/c = 1, and $a/2c$ equal to 0.125 and the second one having $a/2c$ equal to 1.5 whilst the other normalized dimensions remained the same. The wider pit shown in Fig. 4 (a) causes lower values of stress in comparison to the sharper pit presented in Fig. 4 (b). Also, the effect of the pit dissipates in the immediate surrounding of the wider pit whereas around the sharper pit, still a significant range of stress is evident. Concentrated regions of minimum and maximum stress can be observed for the sharper pit; in contrast to the wider pit for which the stresses are more homogeneously distributed over the entire pit wall.

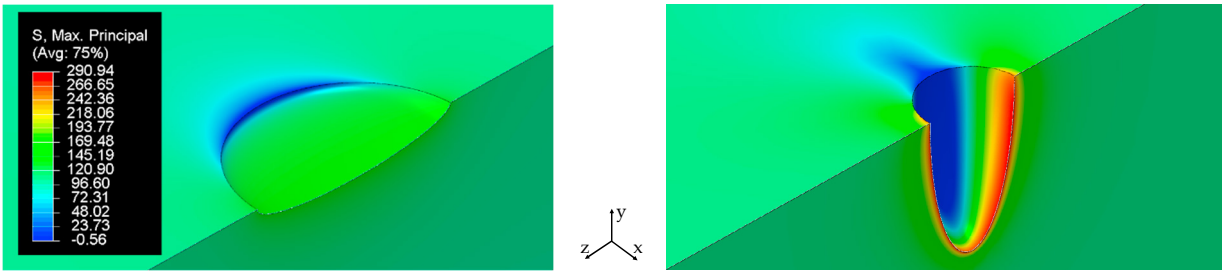

Fig. 4. Maximum principal stress (MPa) for a plate having a pit with a/t = 0.15, b/c = 1.0: (a) $a/2c$ = 0.125 and (b) $a/2c$ = 1.5.

Fig. 5 shows the SCF values versus a/t ranging from 0.01 to 0.2 for $a/2c$ between 0.125 and 1.5 at b/c = 0.1 and b/c = 1. Changes in a/t yield no significant variations in the SCF when $a/t \leq 0.2$. This means that the effect of the localized plate thickness loss is negligible for these shallow pits, which is in agreement with Liang et al. (2019). Similarly, Shojai et al. (2022) have observed negligible SCF variations versus absolute size of pit depth.

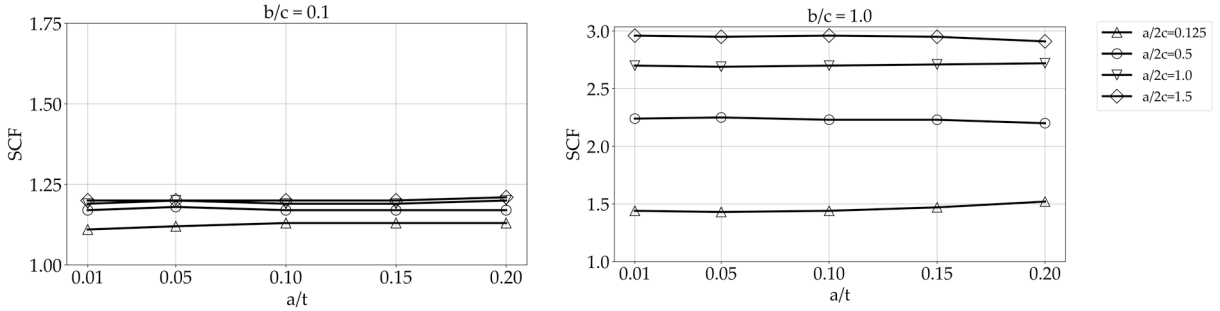

Fig. 5. SCF vs. a/t for a range of $a/2c$ values where (a) b/c = 0.1 and (b) b/c= 1.0.

Both Fig. 5 and Fig. 6 reveal that the SCF increases as the value of $a/2c$ increases. For the widest pits ($a/2c$ = 0.125), the SCF is not significantly different for pits with different pit mouth aspect ratios. The increase in SCF with $a/2c$ is more pronounced for pits with b/c = 1.0. A much smaller increase in SCF is seen for pits with b/c = 0.1; the corresponding SCF curve on Fig. 6 converges to a value of 1.2. On the other hand, the SCF curves do not approach a constant value for b/c = 0.5 and 1.0 within the studied range of $a/2c$. The limited effect of a pit with an extremely narrow mouth (b/c = 0.1) on SCF is most probably the consequence of the loading being parallel to the major axis ($2c$) of the semi-ellipsoidal pit.

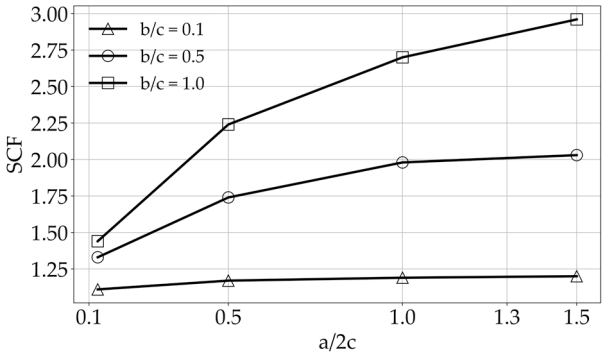

Fig. 6. SCF vs. a/2c for a range of b/c values.

4. Conclusion

A parametric study was carried out to explore the effect of different pit configurations on stress concentration for a plate containing a hemispherical or semi-ellipsoidal pit. Within the studied ranges of geometrical parameters, the results show that the effect of localized plate thickness loss on SCF is negligible for $a/t \leq 0.2$. On the other hand, it was evident that $a/2c$ and b/c significantly affect the SCF. The SCF increases as $a/2c$ and b/c increase. A pit with an elliptical mouth (b/c = 0.1), causes minimum stress concentration even when it is narrow ($a/2c$ > 0.5). Quantifying the stress concentration factor for different pit configurations assists in identifying critical pit shapes and their

susceptibility in transiting into crack(s).

As future work, this study will be extended to a wider range of values for each parameter. Further, the effect of the angle between the pit's length and the loading direction will be quantified.

Acknowledgements

The authors would like to acknowledge the financial support of the Belgian Federal Government through the Energy Transition Fund (ETF).

References

Adedipe, O., Brennan, F., Kolios, A., 2016. Review of corrosion fatigue in offshore structures: Present status and challenges in the offshore wind sector. Renewable and Sustainable Energy Reviews 61, 141–154.

Ahmad, Z., 2006. Principles of Corrosion Engineering and Corrosion Control. Elsevier Ltd.

Ahn, S. -H, Lawrence, F. V., Metzger, M. M., 1992. Corrosion Fatigue of an Hsla Steel. Fatigue & Fracture of Engineering Materials & Structures 15(7), 625–642.

An, L. S., Park, Y. C., Kim, H. K., 2019. A Numerical Study of the Tensile Stress Concentration in a Hemi-ellipsoidal Corrosion Pit on a Plate. International Journal of Steel Structures 19(2), 530–542.

Cerit, M., 2013. Numerical investigation on torsional stress concentration factor at the semi elliptical corrosion pit. Corrosion Science 67, 225–232.

Cerit, M., Genel, K., Eksi, S., 2009. Numerical investigation on stress concentration of corrosion pit. Engineering Failure Analysis 16(7), 2467–2472.

Farhad, F., Smyth-Boyle, D., Zhang, X., 2021. Fatigue of X65 steel in the sour corrosive environment—A novel experimentation and analysis method for predicting fatigue crack initiation life from corrosion pits. Fatigue and Fracture of Engineering Materials and Structures 44(5), 1195–1208.

Huang, Y., Wei, C., Chen, L., Li, P., 2014. Quantitative correlation between geometric parameters and stress concentration of corrosion pits. Engineering Failure Analysis 44, 168–178.

IEA. (2019). World Energy Model. IEA Paris. https://www.iea.org/reports/world-energy-model/stated-policies-scenario

Igwemezie, V., Mehmanparast, A., Kolios, A., 2019. Current trend in offshore wind energy sector and material requirements for fatigue resistance improvement in large wind turbine support structures – A review. Renewable and Sustainable Energy Reviews 101, 181–196.

International Energy Agency, 2019. Offshore Wind Outlook 2019 – Analysis - IEA. https://webstore.iea.org/download/direct/2886?fileName=Offshore_Wind_Outlook_2019.pdf%0Ahttps://www.iea.org/reports/offshore-wind-outlook-2019

Kolios, A., Srikanth, S., Salonitis, K., 2014. Numerical simulation of material strength deterioration due to pitting corrosion. Procedia CIRP 13, 230–236.

Liang, X., Sheng, J., Wang, K., 2019. Investigation of the mechanical properties of steel plates with artificial pitting and the effects of mutual pitting on the stress concentration factor. Results in Physics 14, 102520.

Mehri Sofiani, F., Chaudhuri, S., Elahi, S. A., Hectors, K., De Waele, W., 2023. Quantitative Analysis of the Correlation between Geometric Parameters of Pits and Stress Concentration Factors for a Plate Subject to Uniaxial Tensile Stress. Theoretical and Applied Fracture Mechanics, 104081.

Shittu, A. A., Mehmanparast, A., Shafiee, M., Kolios, A., Hart, P., Pilario, K. (2020). Structural reliability assessment of offshore wind turbine support structures subjected to pitting corrosion-fatigue: A damage tolerance modelling approach. Wind Energy 23(11), 2004–2026.

Shojai, S., Schaumann, P., Brömer, T., 2022. Probabilistic modelling of pitting corrosion and its impact on stress concentrations in steel structures in the offshore wind energy. Marine Structures 84, 103232.

Vukelic, G., Vizentin, G., Ivosevic, S., Bozic, Z., 2022. Analysis of prolonged marine exposure on properties of AH36 steel. Engineering Failure Analysis 135, 106132.

Zhang, J., Hertelé, S., De Waele, W., 2018. A Non-Linear Model for Corrosion Fatigue Lifetime Based on Continuum Damage Mechanics. MATEC Web of Conferences 165, 1–5.